Inorganic Chemistry

Article

pubs.acs.org/IC

Cd_4Cu_7As, The First Representative of a Fully Ordered, Orthorhombically Distorted $MgCu_2$ Laves Phase

Oliver Osters,[†] Tom Nilges,*[,†] Michael Schöneich,[‡] Peer Schmidt,*[,‡] Jan Rothballer,[§] Florian Pielnhofer,[§] and Richard Weihrich*[,§]

[†]Technische Universität München, Department Chemie, Synthese und Charakterisierung innovativer Materialien, Lichtenbergstrasse 4, 85747 Garching, Germany

[‡]Hochschule Lausitz(FH), Fakultät für Naturwissenschaften, Anorganische Festkörper und Materialien, Großenhainer Strasse 57, 01968 Senftenberg, and TU Dresden, Anorganische Chemie, 01062 Dresden, Germany

[§]Universität Regensburg, Institut für Anorganische Chemie Universitätsstrasse 31, 93040 Regensburg, Germany

Supporting Information

ABSTRACT: The ternary Laves phase Cd_4Cu_7As is the first intermetallic compound in the system Cu−Cd−As and a representative of a new substitution variant for *Laves* phases. It crystallizes orthorhombically in the space group *Pnnm* (No. 58) with lattice parameters a = 9.8833(7) Å; b = 7.1251(3) Å; c = 5.0895(4) Å. All sites are fully occupied within the standard deviations. The structure can be described as typical Laves phase, where Cu and As are forming vertex-linked tetrahedra and Cd adopts the structure motive of a distorted diamond network. Cd_4Cu_7As was prepared from stoichiometric mixtures of the elements in a solid state reaction at 1000 °C. Magnetic measurements are showing a Pauli paramagnetic behavior. During our systematical investigations within the ternary phase triangle Cd−Cu−As the cubic C15-type Laves phase $Cd_4Cu_{6.9(1)}As_{1.1(1)}$ was structurally characterized. It crystallizes cubic in the space group $Fd\bar{3}m$ with lattice parameter a = 7.0779(8) Å. Typically for quasi-binary Laves phases Cu and As are both occupying the 16*c* site. Chemical bonding, charge transfer and atomic properties of Cd_4Cu_7As were analyzed by band structure, ELF, and AIM calculations. On the basis of the general formula for Laves phases AB_2, Cd is slightly positively charged forming the *A* substructure, whereas Cu and As represent the negatively charged *B* substructure in both cases. The crystal structure distortion is thus related to local effects caused by Arsenic that exhibits a larger atomic volume (18 Å^3 compared to 13 Å^3 for Cu) and higher ionicity in bonding.

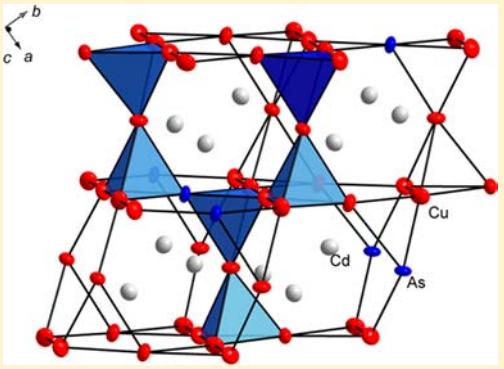

INTRODUCTION

Laves phases are of special interest due to their large flexibility in composition and the resulting variety of physical properties. Beside the full range of addressable magnetic properties of binary and pseudo binary rare earth metal containing C15 Laves phases, used for instance in magneto caloric cooling applications,[1−3] energy related topics like hydrogen storage are also examined and discussed in the literature.[4,5] The well-known basic structure types of Laves phases are the two hexagonal types $MgZn_2$ (C14) and $MgNi_2$ (C36) and the cubic $MgCu_2$ type (C15).[6−8] The conditions for the formation of distinct Laves phases can be understood by two general rules, the geometric and the so-called electronic rule.[7] Thus, a widely examined and therefore huge research field is the topology and chemical bonding in Laves phases which is still intensively discussed in literature.[9−11] The geometric rule is based on the ideal packing of hard spheres leading to an ideal radii quotient of $r_A/r_B = (3/2)^{1/2} = 1.225$. Later this quotient was significantly extended to 1.15−1.30[12] covering most, but not all, of the known Laves phases today. The valence electron concentration (VEC), closely related to the electron concentration and atom size,[10] has been identified as one major aspect for the Laves phase formation. Because of the evident geometric and bonding arguments the application of quantum chemical methods in direct space analyses became very helpful to understand intermetallic compounds from first principles. As one method the Atoms in Molecules (AIM) theory[13] was successfully applied to identify atomic charges and volumes, for example, in Zintl phases[14,15] and metallic bonding in Ni_3S_2.[16] Further the electron localization function/electron localization indicator (ELF/ELI) became very successful to understand bonding in direct space.[17,18] Recently, Grin et al. were able to classify a range of Laves phases systematically by combination of both AIM and ELF analyses.[11]

To the best of our knowledge ordered ternary Laves phases with a distribution of all three elements on distinct positions without mixed occupancies can only be found in the hexagonal

Received: March 9, 2012
Published: July 11, 2012

dx.doi.org/10.1021/ic3005213 | *Inorg. Chem.* 2012, 51, 8119−8127

C14 and C36 structure types and for rhombohedrally distorted C15 Laves phases. Selected examples of each representative are briefly discussed. Considering a general formula AB_2 for binary Laves phases many compounds have been reported. Starting from this formula, Teslyuk introduced two simple variants for substitution in ternary Laves phases:[19] $A_2B_3B^*$ for substitution in the Cu, Zn, or Ni part[19−21] and AA^*B_4 for substitution in the Mg part.[19,22,23] $V(Co_{1-x}Si_x)_2$ with $x = 0.43$ and $x = 0.56$ crystallize in a superstructure of $MgZn_2$-type with a partial ordered substructure of Co and Si, where Co and Si are occupying one edge in the tetrahedron network. In this case, there is still one mixed occupied site left.[24] Na_2Au_3Li is a $MgZn_2$ (C14) type Laves phase where Li and Au are completely ordered.[25] Ordered variants of the $MgCu_2$-type are crystallizing in the Y_2Rh_3Ge structure type,[21] a rhombohedrally distorted variant of a cubic Laves phase. Another example for an ordered variant is the system U_2T_3X (T = Ru, Os; X = Si, Ge).[26]

Our research interest is focused on ternary pnictides of late transition elements. Up to date only a few compounds are known in the binary phase field of Cu−Cd. Beside the copper rich phases $CdCu_2$[27] and Cd_3Cu_4,[28] two cadmium rich compounds Cd_5Cu_2[29] and Cd_8Cu_5[30] were reported. The copper rich phase $CdCu_2$ is a C14 Laves phase with an ordered Cu and Cd substructure, as well as the cadmium rich phase Cd_5Cu_2. Cd_3Cu_4 and Cd_8Cu_5 are showing mixed occupied positions, so no general tendency depending on the elemental contents can be found. The binary arsenic representatives CdAs, $CdAs_2$, Cd_3As_2, $CuAs_2$, Cu_3As, Cu_5As_2 and Cu_3As_4[31−37] are fully ordered, respectively. On investigating the phase field of the system coinage metal (CM)-Cadmium-pnictide, one can find only one intermetallic structure family, (CM)CdSb (CM = Cu, Ag, Au).[38]

In this work we report about the first intermetallic compound Cd_4Cu_7As in the phase triangle Cd−Cu−As and a new orthorhombic substitution variant for Laves phases in the general formula $A_4B_7B^*$. The structural relationship between the cubic C15-type $Cd_4Cu_{6.9(1)}As_{1.1(1)}$ and the orthorhombic title compound will be subsequently elaborated. Recently, the first polyanionic compound in the ternary phase triangle Cd−Cu−As was reported elsewhere.[39] Chemical bonding, charge transfer and atomic properties are analyzed by band structure, ELF, and AIM calculations.

EXPERIMENTAL SECTION

Synthesis. Cd_4Cu_7As was prepared by mixing Cu (Chempur, Powder, 99.9999%), As (Chempur, Pieces, 99.999%) and Cd (Chempur, granules, 99.9999%) in stoichiometric amounts in evacuated silica ampules at temperatures of 1000 °C for 62 h. Phase pure samples were derived after quenching in an ice bath. The reaction batch was homogenized by grinding, sealed in evacuated silica tubes and annealed at 480 °C for 7 days. Crystals were grown evenly distributed in the bulk phase. Arsenic was sublimed twice before usage and stored under dry argon atmosphere afterwards. All other starting materials were used without further purification. For synthesis and characterization of the cubic $Cd_4Cu_{6.9(1)}As_{1.1(1)}$ see Supporting Information.

Phase Analysis. Powder data were collected on a STOE STADI-P diffractometer ($Cu-K_{\alpha1}$ radiation, $\lambda = 1.54051$ Å, Ge-monochromator) with a linear PSD detector. Semiquantitative EDX analysis of selected single crystals was performed on a ZEISS EVO MA10 scanning electron microscope using Cu, Cd, and InAs (As) as standards. The composition (in at-%) was Cu 56(7), Cd 36(3), and As 8(2). These values are in reasonable good agreement with the compositions derived by the X-ray structure refinement and close to the theoretical values in at-% of Cu 58.33, Cd 33.33, and As 8.33 for Cd_4Cu_7As.

Structure Determination. The structure was determined from a suitable single crystal separated from a bulk sample of Cd_4Cu_7As. Intensity data were collected on a IPDS II diffractometer equipped with $Mo-K_\alpha$ radiation ($\lambda = 0.71073$ Å). Absorption was corrected numerically on basis of symmetry equivalent reflections after an optimization of the crystal shape using the Stoe X-red and X-shape programs.[40] The structure was solved by the Superflip routine implemented in the Jana2006 program suite.[41] A chemically meaningful structure model could be derived after checking the systematic extinction in space group *Pnnm* (No 58). Crystallographic data are summarized in Tables 1 and 2.

Table 1. Crystallographic Data of Cd_4Cu_7As Derived from Single Crystal and Powder Data

compound	Cd_4Cu_7As	
method	single crystal	powder sample
temperature (K)	293(2)	298(2)
molar mass (g mol^{-1})	969.4	969.4
crystal size (mm^3)	0.06 × 0.08 × 0.01	
crystal color	dark gray	dark gray
crystal system	orthorhombic	orthorhombic
space group	*Pnnm*	*Pnnm*
lattice parameters		
a (Å)	9.8833(7)	9.9000(1)
b (Å)	7.1251(3)	7.1424(1)
c (Å)	5.0895(3)	5.1019(1)
V (Å^3)	358.40(4)	360.75(1)
Z	2	
ρ_{calc} (g cm^{-3})	8.9798	8.9213
diffractometer	STOE IPDS II	STOE STADI P
radiation	$Mo-K_\alpha$ (0.71073 Å), graphite monochromator	$Cu-K_{\alpha1}$ (1.54051 Å), Ge-monochromator
absorption correction	numerical	none
independent reflections	11780	
R_{int} (all)	4.2	
R_p		8.68
refinement	least-squares on F^2; JANA2006	least-squares on F^2; JANA2006
R ($I > 3\sigma_I$)	1.75	3.07
wR ($I > 3\sigma_I$)	3.77	3.40
R (all)	2.47	3.75
wR (all)	4.10	3.54
parameters	37	48
GOF (all)	1.29	1.01
residual electron density max/min (e Å^{-3})	1.40/−1.54	1.05/-1.13

In order to verify this result we also performed a Rietveld refinement of a sample with the program suite Jana2006.[41] Therefore a powder diffractogram was measured on STOE STADI-P ($Cu-K_{\alpha1}$ radiation, $\lambda = 1.54051$ Å, Ge-monochromator) with a linear position sensitive detector in symmetric transmission mode within a 2Θ range from 5° to 120° and a step width of 0.01°. Measuring time per step was 5 s. The lattice parameters were obtained with the software package WinXpow.[42] The background was fitted by five Legendre polynoms and a pseudo-*Voigt* function.

Detailed information on the structure data can be obtained from the Fachinformationszentrum Karlsruhe, 76344 Eggenstein-Leopoldshafen, Germany (fax (+49)7247−808−666; e-mail crysdata(at)fiz-karlsruhe.de; http://www.fiz-karlsruhe.de/request_for_deposited_data.html) on quoting the depository number CSD 424297 (Cd_4Cu_7As, 293 K).

dx.doi.org/10.1021/ic3005213 | *Inorg. Chem.* 2012, 51, 8119−8127

Table 2. Atomic Coordinates and Isotropic Displacement Parameters of Cd_4Cu_7As at 293 K for Single Crystal Data (Top) and 298 K for Powder Data (Bottom)[a]

atom	x	y	z	U_{iso}	Wyckoff Position
			single crystal data		
Cd1	0.36893(3)	0.65455(5)	0	0.00997(9)	4g
Cd2	0.13315(3)	0.40202(4)	0	0.00983(9)	4g
As1	1/2	1/2	1/2	0.0085(2)	2a
Cu1	1/2	0	0	0.0086(2)	2d
Cu2	0.37862(3)	0.26119(5)	0.24555(6)	0.0099(2)	8h
Cu3	0.24935(5)	0.01873(7)	0	0.0099(2)	4g
			powder refinement data		
Cd1	0.3685(2)	0.6546(2)	0	0.017(2)	4g
Cd2	0.1323(2)	0.4031(3)	0	0.018(2)	4g
As1	1/2	1/2	1/2	0.020(3)	2a
Cu1	1/2	0	0	0.015(3)	2d
Cu2	0.3791(3)	0.2624(3)	0.2462(5)	0.019(2)	8h
Cu3	0.2488(4)	0.0195(5)	0	0.019(2)	4g

[a]All sites are fully occupied within the standard deviations.

Quantum Chemical Calculations. Electronic structure calculations are split into two parts, namely, band structure (reciprocal space) and direct space analysis. The electronic band structure calculations have been performed in the framework of DFT using the full potential local orbital method as implemented in the FPLO program package (version 9.00–34).[43] The band structures and projected density of states were calculated within the generalized gradient approximation (GGA) in the parametrization of Perdew, Burke, and Ernzerhoff (PBE)[44] in a scalar relativistic approximation without the treatment of the spin orbit coupling. The total energy was converged on a k-mesh with 12 × 12 × 12 k-points. Experimental lattice constants and atomic sites were used for Cd_4Cu_7As. Calculations on the compounds Cu_3As, $CdCu_2$, *hcp*-Cd and *fcc*-Cu were also performed with experimental data after[35,27,45,46] for comparison. Cu_3As crystallizes cubic, in space group $I\bar{4}3d$ (no. 220) and its structure is very similar to that of A15-type compounds. Electronic structure and bonding in direct space have been analyzed within the frameworks of the electron localization function (ELF[17]) and the theory of Atoms in Molecules (AIM[13]). Respective electron densities were calculated from all electron basis sets with the CRYSTAL code[47] and analyzed with TOPOND.[48] A net of 48 × 48 × 48 points was applied for the zero-flux-surfaces.

Magnetic Measurements. Magnetic measurements were performed using a MPMS XL5 SQUID magnetometer (Quantum Design) at a constant field of 1000 Oe. The molar susceptibility is temperature independent featuring a value of approximately $\chi_m = 95 \times 10^{-11}$ m^3 mol^{-1} is shown in Supporting Information Figure S1 in good accordance with a Pauli paramagnetic behavior. There is a small curve in the susceptibility which is the result of traces of impurities. Details can be found in the Supporting Information.

Thermoanalytical Investigations. The thermogravimetric (TG) and thermal analysis (DSC) were performed in a simultaneous thermal analyzer (STA 409 Luxx) manufactured by NETZSCH in the temperature range from ϑ = 25 to 1000 °C with a heating rate of 10 °C·min^{-1} in air and argon, respectively. Additionally, a SETARAM Labsys TM analyzer was applied for DSC measurements in the same temperature range from ϑ = 25 to 1000 °C with a heating rate of 10 °C·min^{-1}. In order to avoid oxidation or reduction from the atmosphere and to include the equilibrium vapor pressure of the respective phase, these DSC measurements were done in sealed evacuated silica micro ampules. The temperature of occurring phase transitions and the melting process has been defined by the onset values of the thermal effects, respectively.

RESULTS AND DISCUSSION

Cd_4Cu_7As, the first intermetallic compound in the system Cu–Cd–As, is a new substitution variant for *Laves* phases. The substitution variant can be described as $A_4B_7B^*$ with A = Cd, B = Cu, and B* = As. It crystallizes orthorhombically in space group *Pnnm* (No. 58), with the lattice parameters of *a* = 9.8833(7) Å, *b* = 7.1251(3) Å and *c* = 5.0895(4) Å. In good agreement with common Laves phases Cu and As are forming a three-dimensional network of vertex-linked tetrahedra (Figure 1). Cd forms a diamond-like network (Figure 2) inter-

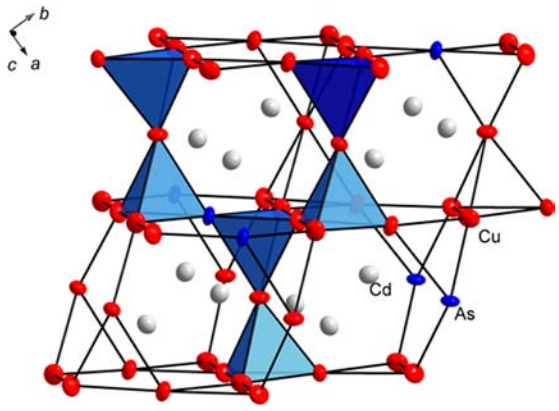

Figure 1. Three-dimensional network of vertex-linked tetrahedra in Cd_4Cu_7As. Displacement parameters are drawn with 90% probability. Black lines are drawn to guide the eyes, to emphasize the tetrahedra and to show sections of the kagome nets formed by Cu and As atoms in the structure.

penetrating the tetrahedron network. There is a systematically replacement of Cu by As, where the pnictide atoms are forming hexagonal packed strands in each Cu layer. Because of this replacement the perfect kagome net in the *ab*-plane is slightly distorted. The short Cd–Cd distances in Cd_4Cu_7As are covering the range of 2.945 Å to 3.102 Å and are therefore comparable with Cd–Cd distances in $CdCu_2$.[27] One of the Cd–Cd distances in Cd_4Cu_7As is slightly enlarged to 3.413 Å due to the substitution of Cu by As in the close neighborhood. This distance is comparable with the Cd–Cd distance in the binary compound CdAs (d(Cd–Cd)= 3.398 Å).[31] All positions are fully occupied within the standard deviations. This is in good accordance to the situation in the binary compounds[27,29,31–37] were Cu, Cd and As are also fully ordered on distinct positions.

dx.doi.org/10.1021/ic3005213 | Inorg. Chem. 2012, 51, 8119–8127

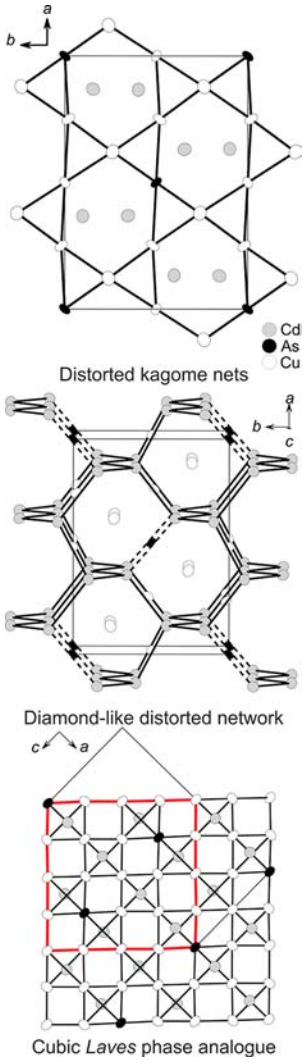

Figure 2. Structure sections of Cd_4Cu_7As. A view onto the (Cu, As) the kagome net in the $a-b$ plane (top) and the distorted diamond-like Cd substructure (middle) is given. The hypothetic elementary cell position of a cubic C15 Laves phase is emphasized in red (bottom). Displacement parameters are drawn with 90% probability. Selected distances are summarized in Table 3.

As subsequently shown As site ordering causes the lowering in symmetry and distortions in metrics compared to known AB_2 Laves phases.

The statement that Cd_4Cu_7As is a new distorted variant of the Laves type can be supported by the description of the structure using the coordination polyhedra principle. Cd is 16-fold coordinated by neighboring atoms forming a Frank-Kasper polyhedron, which is a typical structure element for all of the three basic type Laves phases. Cu and Cd together are forming distorted icosahedra around As with the coordination number 12. Both polyhedra are interpenetrating each other.

Considering the geometric rule a radius quotient of r_A/r_B = 1.23 (with $r_A = r(Cd)$ and $r_B = (7r(Cu) + r(As))/8$)[49] can be calculated for Cd_4Cu_7As, which is the ideal ratio for the formation of Laves phases. The Pearson diagram (Figure 5) shows the ideal radius quotient as a function of A−B and B−B contacts with respect to the atomic radii. Taking the coordination numbers of A (CN = 16) and B (CN = 12) into account, the general empirical eq 1 results[11]

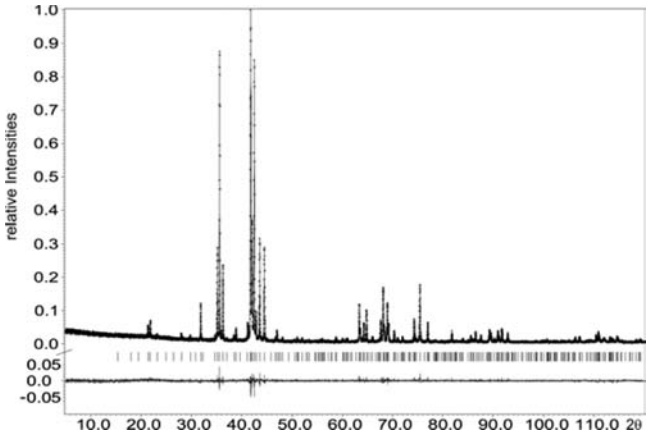

Figure 3. Rietveld plot after a refinement of Cd_4Cu_7As data at 298 K. Relative intensities are plotted against 2θ angles between 5 and 120°. Cu $K_{\alpha 1}$ radiation was used for data collection. Calculated reflection positions and a difference plot are given below the diffractogram, respectively.

Table 3. Selected Distances in Cd_4Cu_7As[a]

atom 1	atom 2	distance (Å)	atom 1	atom 2	distance (Å)
Cd1	Cd2	2.9441(5)	Cu1	Cu3	2.4808(5)
Cd1	Cd2	3.0960(3)	Cu2	Cu3	2.4857(5)
Cd1	Cd1	3.4004(5)	Cu2	Cu2	2.4995(5)
As1	Cu2	2.4518(3)	Cu1	Cu2	2.5425(3)
As1	Cu3	2.4680(5)	Cu2	Cu3	2.5776(5)
Cu3	As1	2.4680(5)	Cu2	Cu2	2.5900(5)

[a] A Rietveld refinement of powder data collected at ambient temperature approves these results.

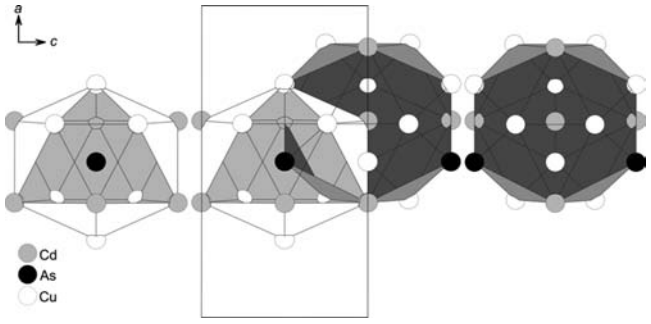

Figure 4. Cd and As coordination polyhedra in Cd_4Cu_7As. Frank−Kasper polyhedra with CN = 16 for Cd (right side) and with CN = 12 for As (icosahedron, left side) are present. Both polyhedra are interpenetrating each other to form the 3D-periodic structure (middle). A not fully filled unit cell is shown for clarity.

$$(2r_A - d_{AA})/2r_B = 0.6450r_A/r_B - 0.7670 \quad (1)$$

d_{AA} is the shortest distance between the A-atoms. Selected Laves phases are shown in Figure 5.

Cd_4Cu_7As perfectly fits to the Pearson relation derived from other Laves phases; it lies for instance in direct neighborhood to the A1-metal phases CsK_2[50] and KNa_2.[52] The title compound shows an electronegativity difference ΔS_{en} = 0.153 according to Sanderson[57] (Electronegativity of Cd, Cu, and As are 1.978, 2.033, and 2.816, respectively) close to $\Delta S_{en}(KNa_2)$ = 0.115 and $\Delta S_{en}(CsK_2)$ = 0.225. Despite of the distortions in the kagome nets and in the diamond-like network in Cd_4Cu_7As there are only contacts between the different atom types.

dx.doi.org/10.1021/ic3005213 | Inorg. Chem. 2012, 51, 8119−8127

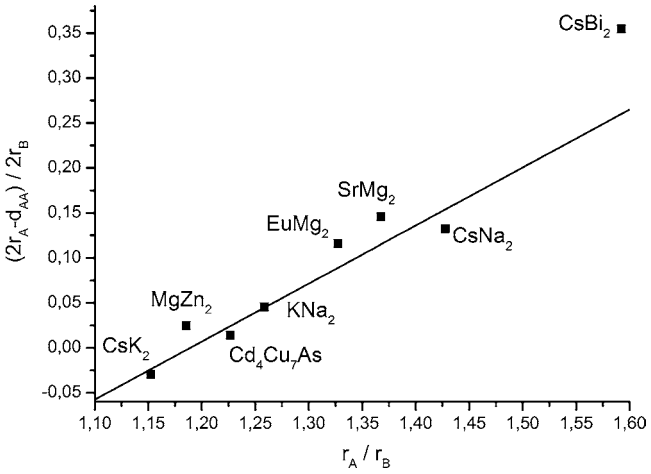

Figure 5. Pearson diagram of selected Laves phases including the title compound Cd_4Cu_7As. Data for the calculations of CsK_2 to $CsBi_2$ are taken from the literature (in order of appearance from bottom left to top right).[50−56] Approximation for the room temperature lattice constants of CsK_2 and $CsNa_2$ are taken from.[12] The slope represents the ideal radii ratio (eq 1).

Electronic Structure. Electronic band structure calculations have been performed for Cd_4Cu_7As in the framework of density functional theory (DFT). The electronic structure coincides for Cd_4Cu_7As and the parent Laves phase $CdCu_2$ in main features as shown by the electronic densities of states (DOS), site projected DOS and fat bands (Figure 6a-c). Because of a nonvanishing at the Fermi-energy (E_F) both compounds are predicted as metals. Both show non bonding and localized Cd-4*d* orbitals in the range of −9.3 to −8.3 eV in accordance with pure hcp-Cd. The main contributions of Cu-3*d* states are located below E_F, so that nonbonding d^{10} states can be concluded, too. However, the splitting of Cu-3d maxima from −1.5 to −4 eV turns out to be characteristic for both Laves phases. It is due to next neighbor interactions (d_{Cu-Cu} = 2.4808(5) Å) that are shorter than in fcc-Cu (2.556 Å[58]).

A first effect of As is detected in the DOS-maximum of As-4s at −12.5 eV that indicates a nonbonding localized lone pair. A different behavior in bonding can be concluded by comparison to Cu_3As, which can serve as a starting material in synthesis. The latter is an A15-type related compound where hybridization of As-4s- and 4p states is found in the same low energy range at −12 eV with higher band dispersion. A second effect arises from As-4p bonding contributions that cause a shift of the states at −2 eV in Cd_4Cu_7As. The As-4p states are broadened over a wide range indicating large overlap in the same fashion as Cu-4s and Cd-5s between the maxima of Cu3d and Cd-4d. One can conclude that the bonding in Cd_4Cu_7As is mainly related to Cu-4s, Cd-5s, and As-4p states. This is underlined by their contributions to bands above and below E_F as shown by fat bands in Figure 6c. The band structure results are consistent with metallic bonding and partial charge transfer as expected for Laves phases. However, completely ionic states cannot be expected due to the various orbital interactions.

Electronic Structure in Direct space. Local bonding and charge transfer turned out as a main criteria for a classification of Laves phases as given in[11] by direct space analysis of the electronic structure. By analysis of the electron localization function[17] and Bader's AIM theory,[13] as recently applied in[59−61] the local electronic structure is related to the initially mentioned geometrical and electronic rules. In the present

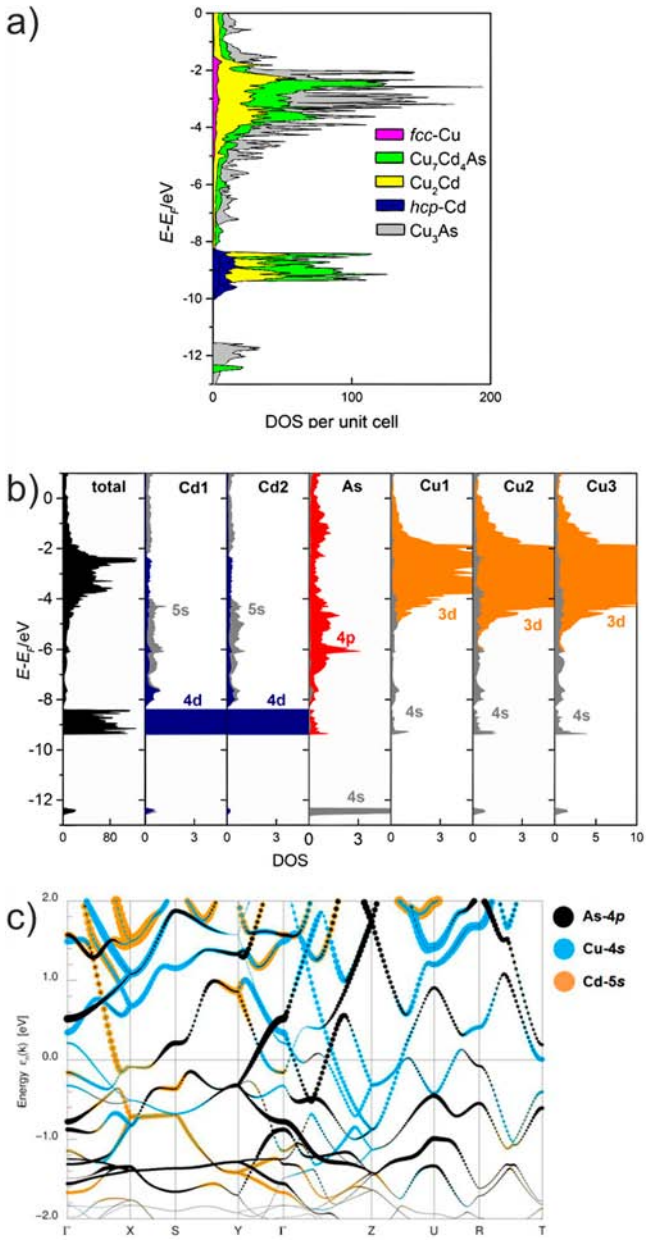

Figure 6. (a) Comparison of the total electronic DOS of Cd_4Cu_7As to Cu_3As, $CdCu_2$, *hcp*-Cd, and *fcc*-Cu (relativistic GGA calculation, citations see Experimental Section). (b) Atomic site projected density of states for Cd_4Cu_7As. (c) Fatband-plot showing bonding and antibonding contributions of As-4p, Cu-4s, and Cd-5s.

case indications for the observed ordering and the structural distortions should be found, too.

In[11] AB_2 Laves phases were classified by multi center bonds within B_4 tetrahedra and toward the A substructure as identified by polysynaptic ELF attractors. No sigma bonds were indicated for the A networks. For Cd_4Cu_7As, similar bonding characteristics are found as visualized by ELF slides within and between the kagome nets of Cu and As (Figure 7). The core electrons of Cu and Cd are signaled by spherical maxima. As the included Cu-3d and Cd-4d shells are not structured they do not participate in bonding.[18] Clearly separated ELF maxima are found in the valence regions, that is, in the middle of Cu_3 triangles (Figure 7, bottom) and around interlayer Cu and Cd atoms (Figure 7, middle). The first belong to polysynaptic ELF

dx.doi.org/10.1021/ic3005213 | Inorg. Chem. 2012, 51, 8119−8127

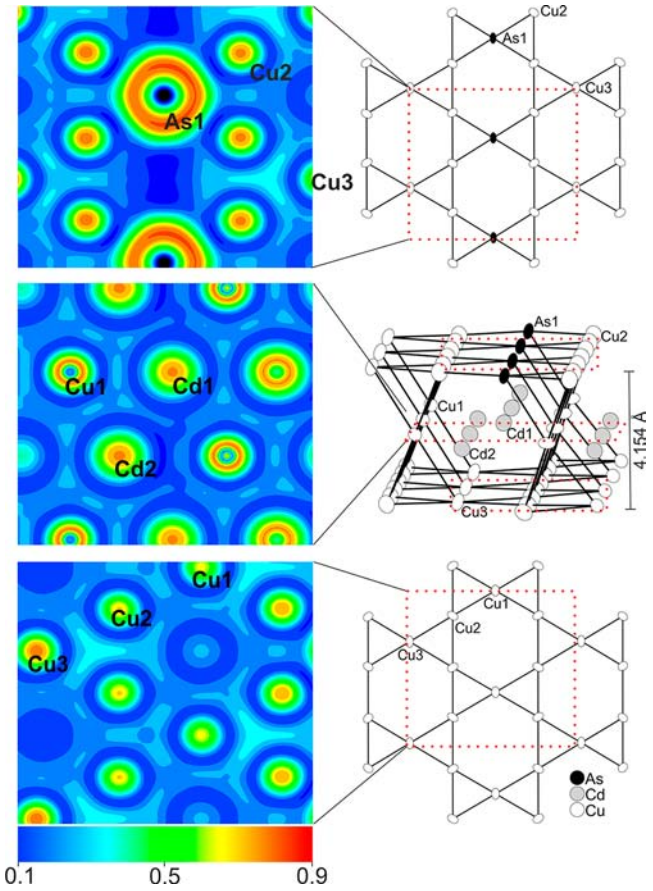

Figure 7. Electron localization function (ELF) of selected structure sections of Cd_4Cu_7As. Each 2D-ELF section (left side) is marked with a dotted line in the structure section on the right-hand side. Details are discussed in the main text.

attractors that are attributed to 4-center bonds in Cu_4 and Cu_3Cd tetrahedra, as also observed from ELI calculations for CsK_2 and $MgCu_2$ type Laves phases in.[11] The second type of ELF attractors in Cd_4Cu_7As are located around Cu and Cd atoms (off-center the kagome layers) that must be related to 3-center-bonds of Cu atoms (B substructure, vertex-linked tetrahedra), pointing toward Cd atoms (*A* substructure, diamond-type network). This feature was also observed for instance in $TiBe_2$.[11] In accordance with the DOS analysis, the As-4s orbitals in Cd_4Cu_7As are spherical and nonbonding (top) indicating that As atoms require more space than Cu atoms (see next chapter). When included in the tetrahedron network they cause a distortion and a shift of the multicenter bonds toward the Cu−Cu edges or even outside the tetrahedra. Furthermore, bonding of As must be done by 4p-orbitals. Similar multicenter bonds in and between kagome nets, but structured and bonding valence electrons were recently observed for S-3sp, Co-3d, and Rh-4d in intermetallic compounds like $In_2Co_3S_2$ and $Sn_2Rh_3S_2$.[60,11]

The second part of the classification of Laves phases is based on the determination of atomic properties and charge transfer according to the AIM theory.[13] Therein, the charge density of chemical compounds is partitioned into atomic basins by the zero-flux condition. From integration of the enclosed charge N_{ZFS} (Table 4) atomic charges $Q_{at} = Z - N_{ZFS}$ (Z = nuclear charge) can be calculated. The obtained negative values for As (−0.5) and Cu (−0.1), but positive for Cd (+0.3) are due to bonding contributions and the difference in electronegativity. Applying the concept of normalized charge transfer the obtained value for Cd_4Cu_7As is as low as in the Laves phase $CdCu_2$ (that was calculated for comparison) but lower than for all Laves phases investigated in ref 11. The Bader basins are space filling, contrary to spherical ionic models. Thus, the discussion of β sphere radii r_β = 1.11 Å (Cu), 1.47 Å (Cd), and 1.34 Å (As) indicates geometrical relations only to a first approximation. To the contrary, integrated atomic volumes serve as a well-defined argument showing that the As atoms ($V_{at.}$ = 18 Å^3) in Cd_4Cu_7As are as large as Cd (18 Å^3) but much larger than Cu (13 Å^3). This emphasizes the structural distortion caused by As. Furthermore, the As atoms cause an asymmetry in charge distribution and in turn atomic dipole moments μ for the Cd (0.13 D), Cu2 (0.17 D), and Cu3 (0.18 D) sites.

Table 4. Results from ZFS Integration Due to the AIM Analysis (Details See Text)

atom	r_β (Å)	V_{at} (Å^3)	Z	N_{ZFS} (e)	Q_{at} (e)	DM_{at} (D)
Cd1	1.47	17.63	48	47.71	+0.29	0.131
Cd2	1.45	17.47	48	47.67	+0.33	0.132
As	1.31	18.04	33	33.49	−0.49	0.005
Cu1	1.11	13.24	29	29.14	−0.14	0.003
Cu2	1.11	13.03	29	29.10	−0.10	0.167
Cu3	1.11	13.20	29	29.10	−0.10	0.189

Finally, the results from AIM and ELF analysis are combined. Within the AIM theory bonds are detected by bond critical points (BCP), for example, Ni−Ni interactions in Ni_3S_2.[16] BCP are (3, −1) saddle points (curvature for 3 directions of the Hessian matrix, sign(x) + sign(y) + sign(z) = −1) of the 3D density and link atoms by bond paths (BP). They appear as necessary condition for any atomic interaction but they do not characterize them.[13] In case of Cd_4Cu_7As BCP are found to interlink Cu and As atoms within the tetrahedron network, as well as Cu and As to Cd atoms (Figure 7). From ELF analyses we know that these bonds have to be characterized as 4- and 3-center bonds. It has been shown that As causes geometrical and bonding distortions which are in general not expected for Laves phases according to the simple empirical rules. So, why does the compound exists? On the basis of the direct space analysis of the electronic structure one must state that As is able to form the required bonds to Cu. This is indicated from both molgraphs of BCP's and atomic basins that have the same dodecahedron-like shape for As and Cu. Both, molgraph and ZFS are determined by the charge density. In a simple way one can conclude that As is able to form bonds and establish the required topology of charge density to stabilize the structure, despite of the violation and distortion of the geometric and electronic rules.

Thermal Analysis. During our research on pnictides we developed thermal and theory based analysis methods to examine and identify stable and metastable compounds.[62,63] Thermal analysis of Cd_4Cu_7As shows the characteristic behavior of incongruent decomposition with a first endothermic effect at 518(2) °C followed by a second endothermic effect at 557(2) °C, Figure 9. The first effect can be assigned to a peritectic or peritectoide decomposition of Cd_4Cu_7As to a cubic C15 Laves phase with a slightly different composition. The second thermal effect occurs during the melt of the cubic phase. The pertinent temperature lies in-between the melting temperatures of the binaries $CdCu_2$ (548 °C[64]) and $CdAs_2$

dx.doi.org/10.1021/ic3005213 | *Inorg. Chem.* 2012, 51, 8119−8127

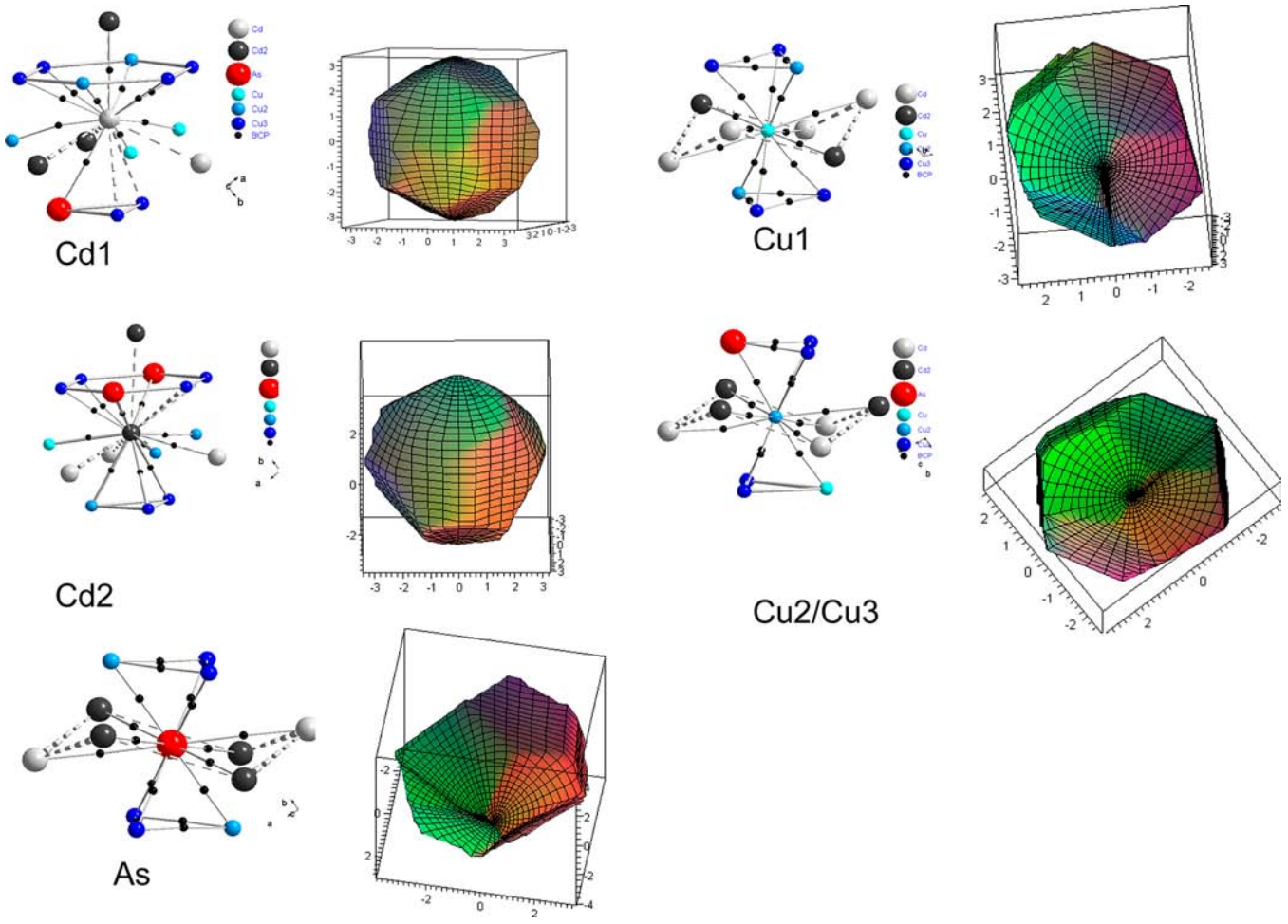

Figure 8. Zero-flux surfaces calculated and visualized for each independent site in Cd_4Cu_7As. A structure section is given on the left-hand side containing the BCP's as small black spheres. Zero-flux surface are shown on the right-hand side of each representation. Values of the zero-flux surfaces are given in Å.

(621 °C[65]), what is assumed as an evidence for the existence of a (partial) homogeneity range in $Cd_4Cu_{8-x}As_x$. Observing the thermal behavior in the cooling mode of Cd_4Cu_7As a strongly divided signal is obtained. Obviously, different stages of incongruent crystallization along the liquidus line occur in the temperature range from 505 to 465 °C. The processes of phase transformation from the cubic toward the orthorhombic phase is completely reversible with a hysteresis of about 50 °C (T_{onset} (transformation) = 465(5) °C).

The cubic phase itself can be derived as a metastable phase at room temperature by quenching of an initial mixture of the nominal composition $Cd_5Cu_{10}As$, which obviously is close to the assumed homogeneity range $Cd_4Cu_{8-x}As_x$ of the cubic phase. A composition of $Cd_4Cu_{6.9(1)}As_{1.1(1)}$ (EDX: $Cd_{4.3(5)}Cu_{7.0(5)}As_{1.0(5)}$) was derived from single crystal X-ray data which will be used in the ongoing discussion. $Cd_4Cu_{6.9(1)}As_{1.1(1)}$ crystallizes cubic in space group $Fd\bar{3}m$ with a lattice parameter of a = 7.0779(8) Å. The cubic phase remains metastable during the heating and melts congruently at 555(2) °C, Figure 9. Steady cooling of the sample results in incongruent decomposition with two exothermic signals. As the lower temperature signal is very small, an incomplete transition can be expected. The measurement in a second run proves the reversibility of phase transitions of the orthorhombic phase Cd_4Cu_7As and the cubic $Cd_4Cu_{6.9(1)}As_{1.1(1)}$. The cubic phase shows almost the same composition than the title compound featuring only very small differences in the negatively charged Cu/As substructure. If this phase is a high temperature polymorph or a second phase with an almost identical composition must be verified in additional experiments. Nevertheless, a group-subgroup relation between both compounds can be formulated substantiating the close relation between the different phases (see Supporting Information). Also, a detailed examination of the composition range $Cd_4Cu_{8-x}As_x$ is still pending. After a preliminary structure determination a mixed occupancy for the Cu and As sites and a full occupancy for Cd has been found. This behavior is common for plethora of quasi-binary C15 Laves phases. As a peculiarity, the cubic C15 structure in $Cd_4Cu_{8-x}As_x$ is realized in contrast to the hexagonal C14 one in $CdCu_2$. Details of the synthesis procedure and the structure determination for the C15 Laves phase can be found in the Supporting Information. TG measurements under an atmosphere of argon show no effects of thermal decomposition forming a gaseous product. That means, the solid phases Cd_4Cu_7As and cubic $Cd_4Cu_{6.9(1)}As_{1.1(1)}$ are stable without evaporation of arsenic. Under an atmosphere of air, the sample is stable up to 400 °C and oxidizes at higher temperatures forming $Cu^{II}As^{III}{}_2O_4$, CuO, and CdO.

dx.doi.org/10.1021/ic3005213 | *Inorg. Chem.* 2012, 51, 8119–8127

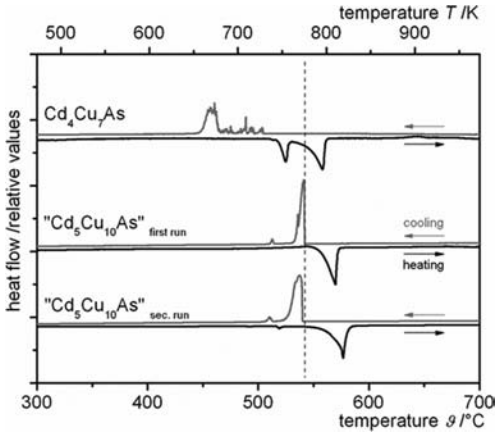

Figure 9. Thermogramm of Cd_4Cu_7As (top section) and the cubic $Cd_4Cu_{6.9(1)}As_{1.1(1)}$ (prepared from a sample with nominal composition $Cd_5Cu_{10}As$ as stated in the middle and bottom part of the Figure). Top part: The first endothermic effect at 518(2) °C can be assigned to a peritectic or peritectoide decomposition of Cd_4Cu_7As to the cubic Laves phase $Cd_4Cu_{6.9(1)}As_{1.1(1)}$. The second effect at 557(2) °C is the melting point of the cubic phase. Middle and bottom part: Two runs of $Cd_4Cu_{6.9(1)}As_{1.1(1)}$ prepared from a sample with nominal composition $Cd_5Cu_{10}As$. Phase analyses substantiated the occurrence of a C15 type Laves phase as the main crystalline fraction (>95%) in this sample.

CONCLUSION

Cd_4Cu_7As represents the first intermetallic compound in the ternary system Cd−Cu−As and a substitution variant of a cubic C15 Laves phase. Starting from the $MgCu_2$ type a fraction of Cu is replaced by As resulting in a new slightly orthorhombically distorted variant. Cu and As are forming a partial negatively charged substructure, interpenetrated by a diamond-like positively charged Cd arrangement. From a formal point of view and in order to substantiate the relation to the Laves phases the base composition AB_2 (e.g., $CdCu_2$) must be multiplied by 4 followed by a replacement of a fraction of the atoms on the B position (Cu) by B* (As). This formalism directly leads to the general formula $A_4B_7B^*$. On the basis of a quasi-binary formalism the title compound has to be written as $CdCu_{1.75}As_{0.25}$. The structure has been determined by single crystal and powder X-ray diffraction experiments, and magnetic measurements proved a Pauli paramagnetic behavior for the title compound.

After detailed quantum chemical calculations based on DFT followed by a Bader and a Mulliken-like population analysis partial atomic charges have been investigated. They showed the expected trend in charges for the different atoms according their electronegativity, respectively. Because of the geometric rules for Laves phases Cd_4Cu_7As is a representative with an ideal radii quotient of 1.23. It also fits perfectly into a so-called Pearson diagram which is based on ideal atom contacts A−B and B−B.

$Cd_4Cu_{6.9(1)}As_{1.1(1)}$, a cubic C15 Laves having an almost identical composition than the title compound can be stabilized after quenching a mixture with the nominal starting composition $Cd_5Cu_{10}As$. In contrast to Cd_4Cu_7As, which is a line compound, the C15 Laves phase is supposed to show a certain phase width.

ASSOCIATED CONTENT

Supporting Information

Electronic files of the crystal structure data (CIF) for both phases, susceptibility measurements, synthesis procedure for the $Cd_4Cu_{6.9(1)}As_{1.1(1)}$ single crystals, tables of atomic coordinates, equivalent isotropic temperature factors and selected distances ($Cd_4Cu_{6.9(1)}As_{1.1(1)}$), and a full group-subgroup relation between the cubic and the new structure variant. This material is available free of charge via the Internet at http://pubs.acs.org.

AUTHOR INFORMATION

Corresponding Author

*Tel. +49 (0)89 289 13110 (T.N.); +49 (0)3573 85827 (P.S.); +49 (0)941 943 4523 (R.W.). Fax +49 (0)89 289 13762 (T.N.); +49 (0)3573 85809 (P.S.); E-mail: tom.nilges@lrz.tum.de (T.N.); peer.schmidt@hs-lausitz.de (P.S.); richard.weihrich@chemie.uni-regensburg.de (R.W.).

Notes

The authors declare no competing financial interest.

ACKNOWLEDGMENTS

O.O. thanks the TUM Graduate School for the financial support. This work was financed by the DFG within the Collaborative Research Centre SPP1415. The authors thank for the opportunity to perform magnetic measurements (Prof. T. F. Fässler and A. Hoffmann, TU München, Germany) and EDX measurements (Prof. R. Pöttgen and C. Schäfer, University of Münster, Germany).

REFERENCES

(1) Hermes, W.; Harmening, T.; Pöttgen, R. *Chem. Mater.* **2009**, *21* (14), 3325.
(2) Sanchez Marcosa, J.; Rodriguez Fernandeza, J.; Chevalier, B.; Bobet, J.-L.; Etourneau, J. *J. Magn. Magn. Mater.* **2004**, *272* (1), 579.
(3) de Oliveira, N. A. *Eur. Phys. J.* **2008**, *B 65*, 207.
(4) Reichert, C.; Kohlmann, H. *Z. Anorg. Allg. Chem.* **2011**, *637* (7−8), 1030.
(5) (a) van Midden, H. J. P.; Prodan, A.; Zupanič, E.; Žitko, R.; Makridis, S. S.; Stubos, A. K. *J. Phys. Chem. C* **2010**, *114* (9), 4221. (b) Kohlmann, H. *J. Phys. Chem. C* **2010**, *114* (30), 13153.
(6) Pearson, W. B. *Acta Crystallogr. B.* **1968**, *24*, 7.
(7) Laves, F. *Naturwissenschaften* **1939**, *27*, 65.
(8) Laves, F.; Wallbaum, H. J. *Z. Anorg. Allg. Chem.* **1942**, *250*, 110.
(9) Johnston, R. L.; Hoffman, R. *Z. Anorg. Allg. Chem.* **1992**, *616*, 105.
(10) Nesper, R. *Angew. Chem.* **1991**, *103*, 805; *Angew. Chem., Int. Ed.* **1991**, *30*, 789.
(11) Ormeci, A.; Simon, A.; Grin, Y. *Angew. Chem.* **2010**, *122*, 9182; *Angew. Chem., Int. Ed.* **2010**, *49*, 8997.
(12) Simon, A. *Angew. Chem.* **1983**, *95*, 94; *Angew. Chem., Int. Ed.* **1983**, *22*, 95.
(13) (a) Bader, R. F. W. *Can. Chem. Rev.* **1991**, *91*, 893. (b) Bader, R. F. W. *J. Phys. Chem. A* **1998**, *102*, 7314.
(14) Ponou, S.; Müller, N.; Fässler, T. F.; Häussermann, U. *Inorg. Chem.* **2005**, *44*, 7423.
(15) Grosch, G. H.; Range, K.-J. *J. Alloys Compd.* **1996**, *235*, 250.
(16) Gibbs, G. V.; Downs, R. T.; Prewitt, C. T.; Rosso, K. M.; Ross, N. L.; Cox, D. F. *J. Phys. Chem. B* **2005**, *109*, 21788.
(17) (a) Becke, A. D.; Edgecombe, K. E. *J. Chem. Phys.* **1990**, *92*, 5397. (b) Savin, A.; Becke, A. D.; Flad, J.; Nesper, R.; Preuss, H.; von Schnering, H. G. *Angew. Chem.* **1991**, *103*, 421;(f) *Angew. Chem., Int. Ed.* **1991**, *30*, 409. (c) Silvi, B.; Savin, A. *Nature* **1994**, *371*, 683. (d) Savin, A.; Nesper, R.; Wengert, S.; Fässler, T. F. *Angew. Chem.*

1997, *109*, 17;(g) *Angew. Chem., Int. Ed.* **1997**, *36*, 1808. (e) Nesper, R.; Wengert, S. *Chem.—Eur. J.* **1997**, *3*, 6.
(18) (a) Kohout, M.; Wagner, F. R.; Grin, Y. *Theor. Chem. Acc.* **2002**, *108*, 150. (b) Wagner, F. R.; Bezugly, V.; Kohout, M.; Grin, Y. *Chem.—Eur. J.* **2007**, *13*, 5724. (c) Kohout, M.; Wagner, F. R.; Grin, Y. *Theor. Chem. Acc.* **2002**, *108*, 150.
(19) Teslyuk, M. Y. *Metallic Compounds with Laves Type Structure*; Nauk: Moscow, 1969.
(20) Teslyuk, M. Y.; Oleksiv, G. I. *Dopob. Akad. Nauk B* **1965**, *10*, 1329.
(21) Cenzual, K.; Chabot, B.; Parthé, E. *J. Solid State Chem.* **1987**, *70*, 229.
(22) (a) Gladyshevskii, E. I.; Kripyakevich, P. I.; Teslyuk, M. Yu. *Dokl. Akad. Nauk SSSR* **1952**, *85*, 81. (b) Osamura, K.; Murakami, Y. *J. Less-Comm. Met.* **1978**, *60*, 311.
(23) Linsinger, S.; Eul, M.; Schwickert, C.; Decourt, R.; Chevalier, B.; Rodewald, U. Ch.; Bobet, J.-L.; Pöttgen, R. *Intermetallics* **2011**, *10*, 1579.
(24) Conrad, M.; Pohling, C.; Webert, H.; Harbrecht, B. *Z. Kristallogr.* **2006**, *221* (5−7), 349.
(25) Range, K. J.; Rau, F.; Klement, U. *Z. Naturforsch. B* **1990**, *45* (9), 1333.
(26) Verniere, A.; Lejay, P.; Bordet, P.; Chenavas, J.; Brison, J. P.; Haen, P.; Boucherle, J. X. *J. Alloy. Compd.* **1994**, *209*, 251.
(27) (a) Kriyakevich, P. I.; Gladyshevskii, E. I.; Cherkashin, E. E.; Hladyshevskii, E. I. *Dokl. Akad. Nauk SSSR* **1952**, *82*, 253. (b) Sulonen, M. S. *Acta Polytech. Scand.* **1962**, *18*, 22.
(28) Kreiner, G.; Schaepers, M. *J. Alloy. Compd.* **1997**, *259*, 83.
(29) Rajasekharan, T.; Schubert, K. *Z. Metallkd.* **1982**, *73*, 262.
(30) (a) von Heidenstamm, O.; Johansson, A.; Westmann, S. *Acta Chem. Scand.* **1968**, *22*, 6. (b) Brandon, J. K.; Brizard, R. Y.; Chieh, P. C.; McMillan, R. K.; Pearson, W. B. *Acta Crystallogr. B.* **1974**, *30*, 1412.
(31) Clark, J. B.; Range, K. J. *Z. Naturforsch. B* **1976**, *31* (2), 158.
(32) Cervinka, L.; Hruby, A. *Acta Crystallogr. B* **1970**, *26*, 457.
(33) (a) Steigmann, G. A.; Goodyear, J. *Acta Crystallogr. B* **1968**, *45*, 1062. (b) Pietraszko, A.; Lukaszewicz, K. *Acta Crystallogr. B* **1969**, *25*, 988.
(34) Naud, J.; Priest, P. *Mater. Res. Bull.* **1972**, *7*, 783.
(35) Iglesias, J. E.; Nowacki, W. *Z. Kristallogr.* **1977**, *145*, 334.
(36) Liebisch, W.; Schubert, K. *J. Less-Common Met.* **1971**, *23*, 231.
(37) Blendl, C.; Range, K. J. *Z. Kristallogr.* **1982**, *159*, 17.
(38) Belotskii, D. P.; Makhova, M. K.; Galichanskii, V. G.; Kotsyumakha, M. P. *Izv. Akad. Nauk SSSR, Neorg. Mater.* **1970**, *6*, 1593.
(39) Osters, O.; Nilges, T. *Acta Crystallogr. E* **2011**, *67*, i62.
(40) *STOE XArea*, version 1.56; STOE & Cie GmbH: Darmstadt, Germany, 2011.
(41) Petricek,V.; Dusek, M.; Palatinus, L. *Jana2006. The Crystallographic Computing System*; Institute of Physics: Praha, Czech Republic, 2006.
(42) *STOE WinXPOW*, version 2.08; STOE & Cie GmbH: Darmstadt, Germany, 2008.
(43) Koepernik, K.; Eschrig, H. *Phys. Rev. B* **1999**, *59*, 1743.
(44) Perdew, J. P.; Burke, K.; Ernzerhof, M. *Phys. Rev. Lett.* **1996**, *77*, 3865.
(45) Hull, A. W.; Davey, W. P. *Phys. Rev.* **1921**, *17*, 266; *Phys. Rev.* **1921**, *17*, 549; *Z. Phys. Chem.-Leipzig* **1924**, *109*, 183.
(46) Bragg, W. L. *Philos. Mag.* **1914**, *28* (6), 255; *Ann. Phys.-Leipzig* **1922**, *69* (4), 59; *Phys. Z.* **1922**, *23*, 114.
(47) Dovesi, R. *crystal98 User's Manual*; University of Torino: Torino, Italy, 1998.
(48) Gatti, C. *TOPOND96 User's Manual*; CNR-CSRSRC: Milan, Italy, 1997.
(49) Pauling, L. *J. Am. Chem. Soc.* **1947**, *69* (3), 542.
(50) Simon, A.; Brämer, W.; Hillenkötter, B.; Kullmann, H. J. *Z. Anorg. Allg. Chem.* **1976**, *419*, 253.
(51) Lieser, K. H.; Witte, H. *Z. Metallkd* **1952**, *43*, 396.
(52) Laves, F.; Wallbaum, H. J. *Z. Anorg. Allg. Chem.* **1942**, *250*, 110.
(53) Klemm, W.; Kock, H.; Mühlpfordt, W. *Angew. Chem.* **1964**, *76*, 862; *Angew. Chem., Int. Ed.* **1964**, *3*, 704.
(54) Laves, F.; Hellner, E. *Z. Kristallogr.* **1943**, *105*, 134.
(55) Simon, A.; Ebbinghaus, G. *Z. Naturforsch. B* **1974**, *29*, 616.
(56) Emmerling, F.; Längin, N.; Petri, D.; Kroeker, M.; Röhr, C. *Z. Anorg. Allg. Chem.* **2004**, *630*, 171.
(57) Sanderson, R. T. *J. Am. Chem. Soc.* **1983**, *105*, 2259.
(58) Donohue, J. *The Structures of the Elements*; Wiley & Sons: Florida, U.S.A., 1982; p. 221.
(59) Pielnhofer, F.; Bachhuber, F.; Rothballer, J.; Peter, Ph.; Schappacher, F. M.; Pöttgen, R.; Weihrich, R. *Z. Anorg. Allg. Chem.* **2012**, *635*, 2410.
(60) Anusca, I.; Schmid, A.; Peter, Ph.; Rothballer, J.; Pielnhofer, F.; Weihrich, R. *Z. Anorg. Allg. Chem.* **2009**, *635*, 2410.
(61) Bachhuber, F.; Anusca, I.; Rothballer, J.; Pielnhofer, F.; Peter, P.; Weihrich, R. *Solid State Sci.* **2011**, *13*, 337.
(62) Schmidt, P.; Schöneich, M.; Bawohl, M.; Nilges, T.; Weihrich, R. *J. Therm. Anal. Calorim.* **2012**, DOI: 10.1007/s10973-011-2107-3.
(63) Osters, O.; Nilges, T.; Bachhuber, F.; Pielnhofer, F.; Weihrich, R.; Schöneich, M.; Schmidt, P. *Angew. Chem.* **2012**, *124* (12), 3049; *Angew. Chem., Int. Ed.* **2012**, *51* (12), 2994.
(64) *Binary Alloy Phase Diagrams*, Sec. Edt., Ed. Massalski, T. B.; ASM International, Materials Park, OH, 1990, *2*, 973.
(65) *Binary Alloy Phase Diagrams*, Sec. Edt., Ed.Massalski, T. B.; ASM International, Materials Park, OH, 1990, *1*, 265.